

An innovative clay *meta*Brick-based motif to enhance thermal and acoustic insulation

Brahim Lemkalli^{a,*}, Saad Bensallam^b, Muamer Kadic^c, Sébastien Guenneau^{d,e}, Hicham Jakjoud^f, Abdellah Mir^g, Younes Achaoui^a

^aLaboratory of Optics, Information Processing, Mechanics, Energetics and Electronics, Department of Physics, Moulay Ismail University, B.P. 11201, Zitoune, Meknes, Morocco

^bHassania School of Public Works, Casablanca, Morocco

^cUniversité de Franche-Comté, institut FEMTO-ST, UMR 6174, CNRS, 25000 Besançon, France

^dThe Blackett Laboratory, Physics Department, Imperial College London, SW7 2AZ, London, UK

^eUMI 2004 Abraham de Moivre-CNRS, Imperial College London, SW7 2AZ, London, UK

^fLaboratory of Energy Engineering, Materials and Systems, National Schools of Applied Sciences, Ibn Zohr University, Agadir, Morocco

^gDepartment of Physics, Moulay Ismail University, B.P. 11201, Zitoune, Meknes, Morocco

Abstract

Metamaterials have gained popularity in recent years as a promising avenue for producing innovative materials with distinctive properties that offer unprecedented features. In this study, we address the thermal and acoustic challenges of building materials. We numerically and experimentally investigate a clay *meta*Brick, which is an innovative metamaterial design based on the existing hollow brick that has shown strong sound and thermal performances. We evaluate the acoustic and thermal characteristics of the clay *meta*Brick, including sound transmission and heat resistance, using the finite element method. Furthermore, we validate the results experimentally by investigating the behaviors of the wall built on *meta*Bricks in two tests: sound and thermal. We contrast the findings of the *meta*Brick based wall with performances of a standard hollow brick wall. The *meta*Brick offers enhanced acoustic and thermal insulation properties compared to the standard brick, with a compressive strength above standards required in the building materials.

Keywords: Metamaterials; Helmholtz resonators; Clay *meta*Brick; Sound insulation; Thermal insulation

1. Introduction

Recently, in response to climate change and noise pollution, building materials with particular characteristics that may be employed to provide efficient heat and sound insulation have become necessary [1–3]. These materials are crucial for decreasing energy consumption while enhancing comfort and safety in both residential and commercial environments [4–6]. Most studies have focused on improving the thermal and acoustic insulation of hollow clay bricks, which are the most commonly used construction materials due to their durability, low cost, and availability [7]. In

*Corresponding author

Email address: brahim.lemkalli@edu.umi.ac.ma (Brahim Lemkalli)

this regard, several approaches have been explored to increase the insulating properties of clay bricks. A common method is to add insulation materials, such as phase change materials, to the structure of the bricks to improve their thermal resistance [8–14]. Other research looked at the use of nanocrystalline aluminum sludge to increase the thermal efficiency of perforated clay bricks [15]. Acoustically, several clay bricks with distinct hollow cores were analyzed [16]. Furthermore, it has been reported that additional layers to the hollow bricks improve their acoustic performance [17]. Another method is to change the structure of the bricks themselves, for example, by modifying the geometry of the air holes [18]. Besides these approaches, clay brick still has limitations in terms of both thermal and acoustic insulation properties. Therefore, additional advancement in the development of more efficient insulation techniques remains necessary.

To control both phenomena, sound and heat, multi-functional metamaterials that combine these two physics are required. Metamaterials are man-made materials that have been developed to exhibit unique features that are not naturally disposable [19, 20]. These materials have the potential to provide simultaneous heat and sound insulation, which can significantly improve energy efficiency and comfort in buildings and other applications. On the one hand, acoustic metamaterials are a type of metamaterials that are used to manipulate sound waves [21]. In order to improve sound insulation, a variety of resonators with different characteristics are being studied, including phononic crystals with a Bragg-based bandgap [22, 23], free-standing [24–28], space coiled [29, 30], Fabry-Perot [31], quarter-wavelength [32], and Helmholtz resonators [33–35]. By exploiting the special characteristics of acoustic metamaterials, it is feasible to design metamaterials that effectively block, absorb or deflect sound waves. On the other hand, thermal metamaterials have been designed to manipulate heat flow [36, 37]. These materials have unique thermal properties that enable unprecedented control over heat transfer. By engineering thermal metamaterials, it is possible to create materials that can efficiently trap or release heat, which makes them useful for applications such as thermal insulation [38].

In this paper, we suggest a new design for a hollow clay brick called a "*meta*Brick," where the word "meta" refers to the concept of metamaterials. The *meta*Brick is built on Helmholtz resonators, which are designed to reduce the transmission of both sound and heat. Helmholtz resonators are more interesting for creating low-frequency sound insulation [39], which is the straightforward reason why we use Helmholtz resonators. To evaluate the acoustic and thermal characteristics of the *meta*Brick, we combine the finite element approach with experiments. The results of the *meta*Brick are compared to those of the standard clay brick. The first section places a strong focus on the numerical performance analysis of the bricks. The second section is dedicated to empirically evaluating the effectiveness of a wall made of *meta*Bricks, which involves measuring the walls' thermal, acoustic and mechanical properties.

2. Characteristics of the *meta*Brick

To contribute to the development of the building materials, we have developed the hollow bricks into novel bricks called *meta*Bricks, referring to the exotic behavior of metamaterials applied to the specific case of standard hollow bricks. The *meta*Brick design consists of an array of brick-shaped units with hollow cores, similar to a standard brick, but with the addition of slits at the top and the bottom of the standard hollow brick, as shown in Fig. 1. These features create Helmholtz resonators within the *meta*Brick, which can attenuate sound and reduce heat transfer. The dimensions of the *meta*Brick used in this study are 10 cm in width, 25 cm in length, and 20 cm in height. The slits

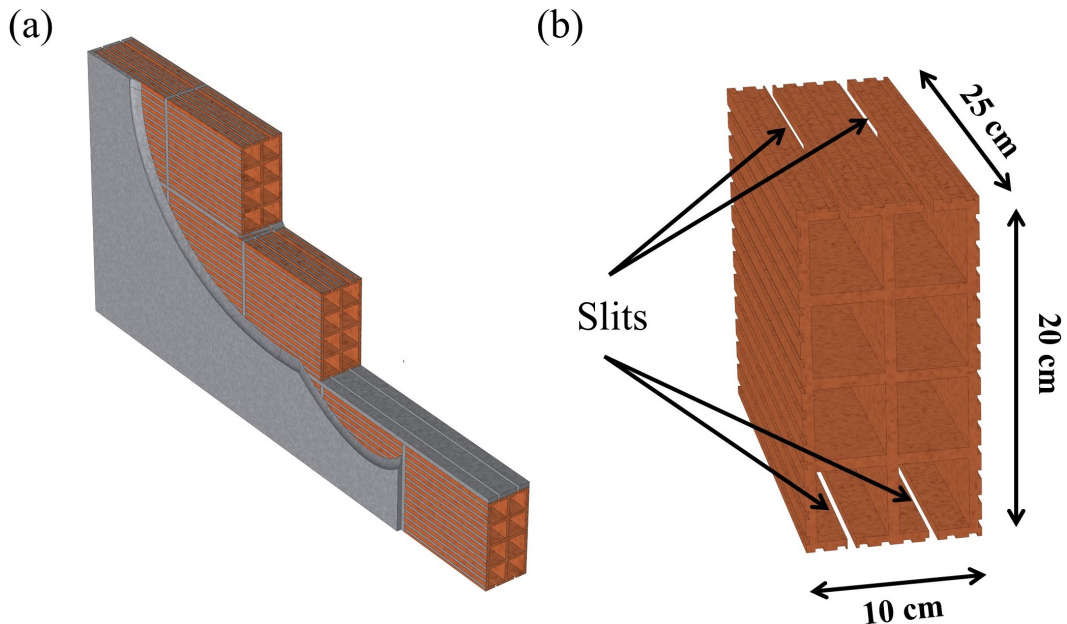


Fig. 1. Schematics of the Clay hollow *metaBricks*. (a) Wall made of clay *metaBricks* and mortar. (b) Clay hollow *metabrick*.

Table 1: Building *metaBrick* mechanical and thermal properties

Material	Young modulus GPa	Poisson's ratio	Density kg/m ³	Thermal conductivity W/(mK)	Specific heat J/(kgK)	Sound speed m/s
Clay	17	0.2	2000	0.5	900	-
Mortar	25	0.2	2300	1.8	880	-
Air	-	-	1.21	0.025	1005.3	343

on the top and bottom of the *metaBrick* are 0.5 cm in width and 25 cm in length. The *metaBrick*-based wall is illustrated in Fig. 1(a). The material parameters used in this study are depicted in Table 1.

To comprehensively characterize the acoustic and thermal performances of the *metaBrick*, we use 2D simulations based on the finite element method. For sound transmission, we use a common method that is based on the excitation of an acoustic plane wave and measures the acoustic transmission of the brick. The response of the brick to the plane wave can provide insights into its ability to absorb, reflect, or transmit sound, which is critical for designing structures that are acoustically comfortable and meet regulatory standards. Similarly, for thermal study, a sinusoidal temperature is often applied to the brick to simulate various thermal conditions. The brick's response to this temperature change is then analyzed to evaluate its thermal performance, including its ability to insulate heat or regulate temperature.

2.1. Acoustic response

The numerical model used in the acoustic study is based on solving the acoustic wave propagation equations in both air and solid. Sound waves in air are governed by equation 1 for differential pressure p . The solid is considered as an isotropic linear elastic material, and the propagation of acoustic waves is determined by solving the weak formalism of the time-harmonic Navier equation (2).

$$\nabla \cdot \left(\frac{1}{\rho_{air}} \nabla p \right) + \frac{\omega^2}{\rho_{air} C^2} p = 0, \quad (1)$$

$$\frac{E}{2(1+\nu)} \left(\frac{1}{1-2\nu} \nabla(\nabla \cdot \mathbf{u}) + \nabla^2 \mathbf{u} \right) = -\omega^2 \rho_s \mathbf{u}, \quad (2)$$

where p is the acoustic pressure, \mathbf{u} is the displacement vector, ρ_{air} and ρ_s are the densities of air and solid, respectively. C is the speed of sound in air, ω is the angular frequency of the acoustic wave, E is the Young's modulus, and ν is the Poisson's ratio.

In order to simulate the normal incident sound wave, a plane wave radiation boundary condition was utilized, and Perfectly Matched Layers (PMLs) were placed at both extremities of the medium to limit spurious reflections, as depicted in Fig. 2(a). Furthermore, the Floquet-Bloch periodic conditions are applied on the top and bottom of the bricks. We calculate the transmission in the frequency range (20 Hz to 5 kHz) for each brick, using equation (3).

$$Transmission = 20 \times \log_{10} \left(\frac{|p_t|}{|p_i|} \right), \quad (3)$$

where p_i and p_t are the incident and transmitted pressures, respectively.

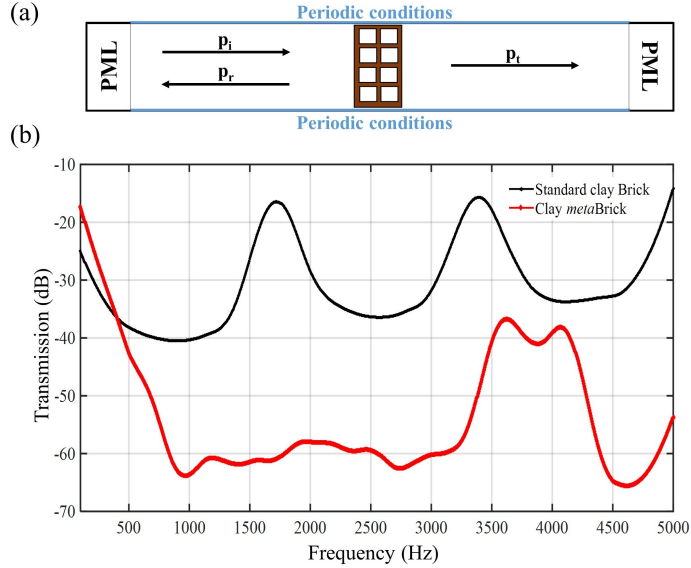


Fig. 2. Sound Transmission. (a) Numerical model. (b) Transmission curves for the two types of bricks: the *meta*Brick portrayed in the red curve and the standard brick represented by the black curve.

Fig. 2(b) displays the sound transmission of two types of bricks, the standard brick (black curve) and the *meta*Brick (red curve), across a wide range of frequencies. It is evident that the standard brick has a higher sound transmission compared to the *meta*Brick, which is due to the tiny guide between the two successive bricks creating a Fabry-Perot resonator that has a resonance at $n\lambda/2$ (where λ is the wavelength). The presence of slits, i.e., Helmholtz resonators, reduces the sound transmission by 20 dB across a broad frequency range from 500 Hz to 3500 Hz, beyond which the limit of diffraction becomes apparent. The superior acoustic insulation properties of the *meta*Brick are clearly demonstrated through the transmission curve, as it effectively attenuates sound waves more than the classical brick. This finding, which applies without mortar, is of practical significance as it highlights the importance of reducing sound transmission through building materials to create acoustically comfortable structures that comply with regulatory standards. The response of the two

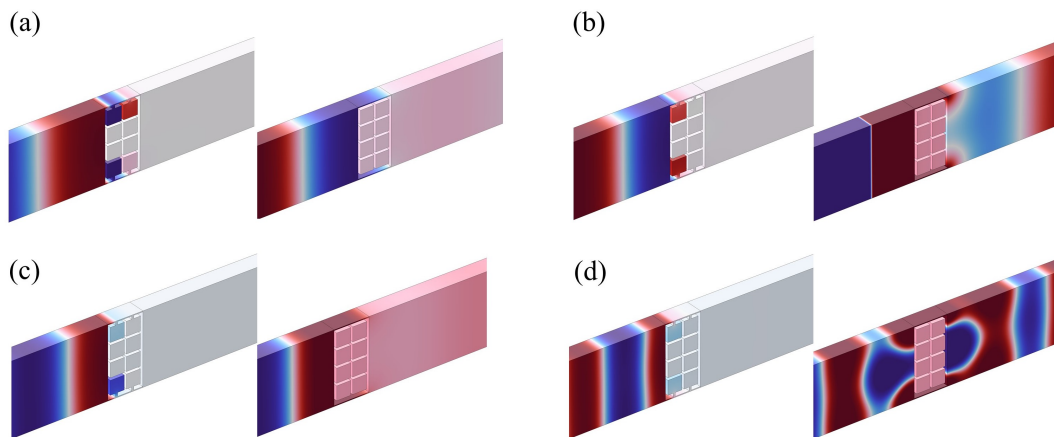


Fig. 3. Screenshots of the acoustic response of the standard brick (right) and the *meta*Brick (left). (a) At a frequency of 500 Hz. (b) At a frequency of 671 Hz. (c) At a frequency of 793 Hz. (d) At a frequency of 1500 Hz.

types of bricks to plane wave excitation is further analyzed using screenshots shown in Fig. 3. The screenshots provide a visual representation of the bricks' reactions to the plane wave at different frequencies and demonstrate that the *meta*Brick attenuates the sound wave more efficiently than the standard brick. This observation reinforces the conclusion that the *meta*Brick has superior acoustic insulation properties. The figure particularly highlights the energy trapping inside the Helmholtz resonators in the metabricks at different frequencies, unlike the classical ones, in which cavities play no particular role in the acoustic insulation. In summary, the study provides valuable insights into the acoustic performance of two types of brick and highlights the advantages of using the *meta*Brick for acoustic insulation applications.

2.2. Thermal response

For the thermal analysis, the heat transfer in solids and fluids equations was utilized to characterize thermal insulation through the bricks. By solving the transient heat equation (4), the temperature distribution within the unit cells is calculated. The methodology is based on applying a sinusoidal temperature within a 24-hour period ranging between 0 and 50 °C and determining the inner temperature of unit cells, as shown in Fig. 4(a). To accomplish this, the terminal boundaries of the configuration are exposed to ambient temperature, which is set to $T_{amb} = 25$ °C. The outer

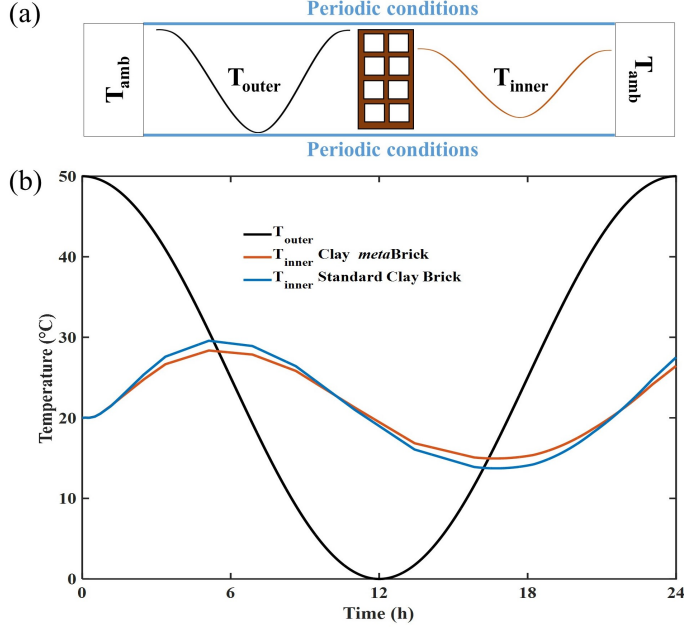


Fig. 4. The temperature response. (a) Numerical model. (b) Temperature evolution for the two types of bricks: the standard brick is represented by the blue curve, the *meta*Brick by the red curve, and the outer temperature by the black curve.

boundary of cells is vulnerable to the outer temperature $T_{out}(t)$, which describes the temperature variation over a 24-hour period with the expression $T_{out} = 25\sin(\frac{2\pi}{24}t) + 25$ °C. Furthermore, the periodicity conditions are applied in the top and bottom of bricks.

$$k_i \Delta T = \rho_i c_i \frac{\partial T}{\partial t}, \quad (4)$$

where i indicates air or solid, k_i , ρ_i and c_i are the thermal conductivity, the density and the specific heat, respectively.

Fig. 4(b) reports a comparative analysis of the thermal properties of two types of bricks, namely the standard brick (curve in red) and the *meta*Brick (curve in blue). The results demonstrate that the *meta*Brick exhibits superior thermal insulation properties compared to the standard brick. Specifically, the *meta*Brick displays lower temperature values than the standard brick, indicating a greater capacity for retaining heat.

The superiority of the *meta*Brick's thermal insulation properties is further supported by the screenshots provided in Fig. 5, which depict the temperature distribution across the bricks over time. The screenshots show that the *meta*Brick retains heat more effectively than the standard brick, thereby reducing the need for additional heating or cooling.

The 2D numerical model provided a useful tool to further investigate the performance of the *meta*Brick design and its potential to reduce both sound and heat propagation. The simulations performed with the model allowed for the exploration of one scenario where one unit cell represents a brick without mortar and is infinite in the out-of-plane, while in reality the bricks are finite and constructed in a wall with mortar, which would have been difficult or impossible to achieve in the

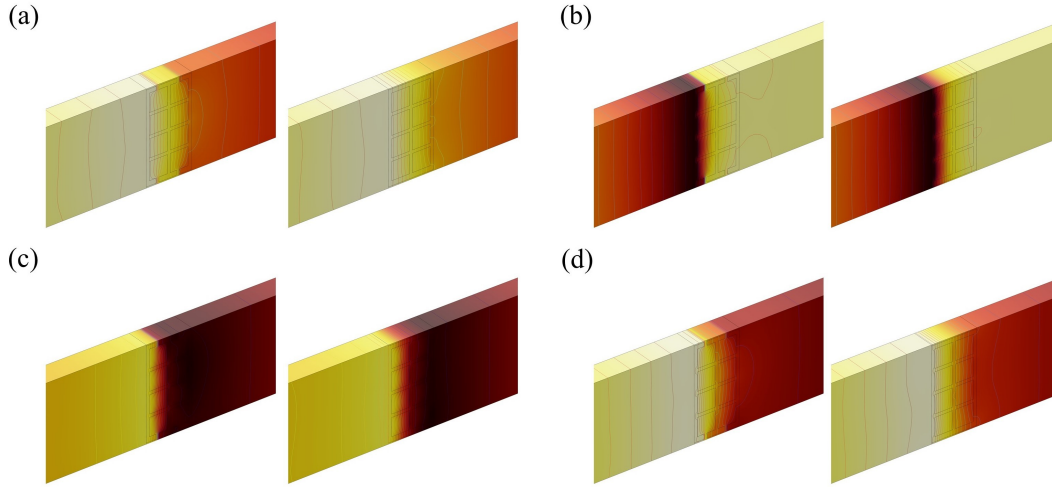


Fig. 5. Screenshots of the temperature contour response of the standard brick (right) and the *metaBrick* (left). (a) After 4 hours of exposure. (b) After 10 hours of exposure. (c) After 18 hours of exposure. (d) After 24 hours of exposure.

2D simulations. In the next section, to make the investigation more realistic, the performance of a 3D wall made of bricks and mortar is reported. In order to have a deeper understanding of the acoustic and thermal behaviors of the *metaBrick* wall, the data obtained from the numerical simulations will be compared to with the data from the experiment.

3. Characteristics of a *metaBrick* wall

Following the 2D numerical simulations that demonstrated the superior acoustic and thermal properties of the *metaBrick*, our subsequent step involved determining its performance through both experimental and numerical investigations. We constructed two identical walls, one built using the *metaBrick* and the other using standard brick. The walls were exposed to controlled acoustic and thermal conditions, and we recorded the responses across each wall. By comparing the experimental data obtained from the two walls, we ascertained the performances of the *metaBrick* wall. Furthermore, numerical simulations were carried out to study the behavior of both walls. The results obtained from the simulations were compared with the experimental data to validate the accuracy of the simulation models and gain further insight into the acoustic and thermal properties of the walls. Through the combined approach of experimental and numerical investigations, we were able to obtain a comprehensive understanding of the properties of the *metaBrick* wall and its advantages over standard brick walls. In Fig. 6, several images of the *metaBrick* used in our experimental tests are displayed. The images illustrate the top and side views of the *metaBrick*, side-by-side, allowing for a direct visual comparison of their geometrical attributes. The *metaBrick*'s unique design and composition can be observed, which include a mixture of various materials to enhance its thermal properties. These images provide a visual representation of the experimental setup and the materials used, which can help to understand the experimental results presented further down in this document.

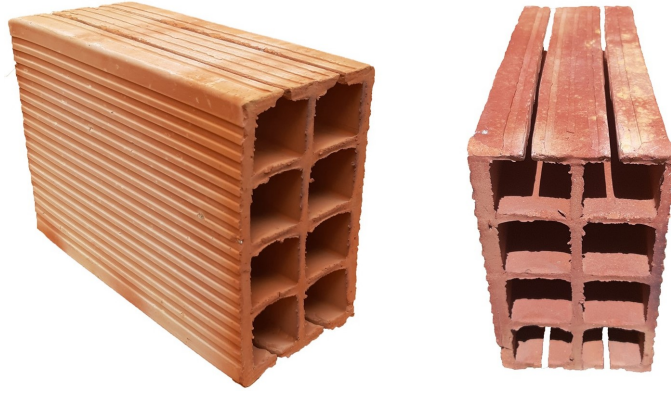


Fig. 6. Clay hollow *metabrick* experimental pictures, with a side view on the left and a top view on the right.

3.1. Experimental and numerical setups

The experimental setups used in this study have been mounted to investigate the acoustic and thermal behaviors of the novel *metaBrick* and compared to a standard brick. The schematics of these setups are illustrated in Fig. 7(a) and (b). Thus, these setups were composed of a double steel box, as depicted in Fig. 7(c) and (d), in which one side is left open to be filled with the brick-based walls. The walls were constructed using the *metaBrick* and the standard brick.

For the acoustic study, a loudspeaker was used as the excitation source, and the signals were detected using a microphone that was placed inside the iron box. The theoretical chirp is used to generate the sound, which is at a sufficiently high amplitude in order to get a sound pressure level in the receiving room without the influence of background noise, and the frequency response covers the relevant measurement range, which is at least from 50 Hz to 5000 Hz.

The sound pressure level in the box is measured with a calibrated measurement microphone. The microphone was positioned in a fixed location throughout the experiment and numerical test because the sound pressure level in the box varies from one point to another, even in an ideal diffuse sound field. For that, we have conserved the same point for both experimental and numerical tests. The collected data, which represents the pressure in function of time, is processed with the fast Fourier transformation to the amplitude of the sound with the expression $amplitude = 20 * \log_{10}(p)$. The results of this study are illustrated in Fig. 8.

In the thermal study, a heat source was used as the excitation source. Both walls were exposed to an outer temperature of 96 °C for 600 minutes in an ambient temperature of 25 °C, and the temperature fluctuations were measured using infrared thermometers that were positioned at a fixed distance from the wall surface on both sides, the inner side and the outer side. The thermometers were used to measure the temperature evolution of the wall at different time intervals. The results of this study are illustrated in Fig. 9.

The experimental setup allowed for accurate and reliable measurements of the acoustic and thermal behaviors of both the *metaBrick* and the standard brick. In addition to the experimental analysis, a numerical model was used to further investigate the acoustic and thermal behaviors of the *metaBrick* design. The numerical model was constructed using the same dimensions and setup as used in the experimental study to ensure consistency and accuracy of the results. Both numerical and experimental setups are based on the same approaches. The objectives of these approaches are

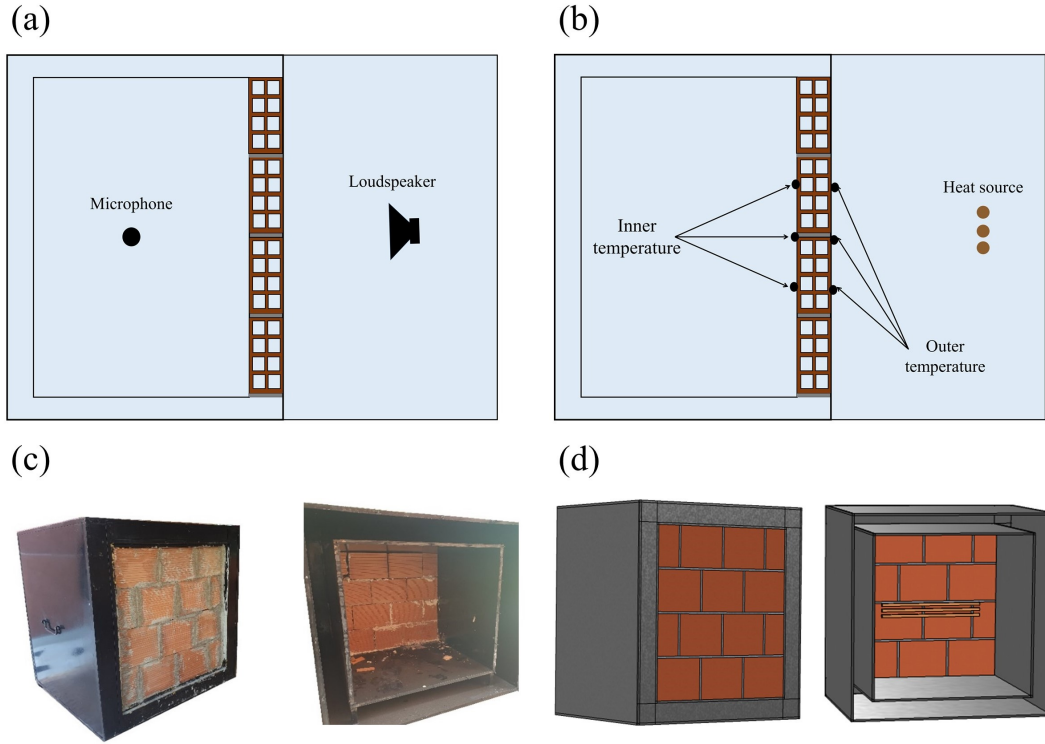


Fig. 7. Setups for numerical and experimental analysis. (a) An acoustic setup for measuring sound transmission amplitude in both experimental and numerical studies. (b) The thermal setup to determine the inner temperature in both experimental and numerical studies. (c) The experimental box with a wall. (d) The numerical box with a wall.

to fit the numerical and experimental results and gain a better understanding of the responses of the proposed clay brick. The experimental results were compared with the numerical simulations to validate the accuracy of our modeling approach.

3.2. Results

The results obtained from the acoustic analysis provided valuable insights into the effectiveness of the *meta*Brick design in attenuating sound, as shown in Fig. 8. The analysis of the four signals obtained, namely the excitation chirp signal (in violet), the measured excitation signal without walls (in blue), steel box sound transmission (in pink), standard brick sound transmission (in black), and *meta*Brick signal transmission (in red), enabled a comparison of their respective acoustic behaviors. The numerical and experimental results are presented in Fig. 8(a) and (b), respectively. It is clearly seen that the numerical results and the experimental results are in good agreement; in what follows, we interpret both results together. The steel box transmission signal indicated a very weak transmission amplitude in the frequency range of 100 to 5000 Hz. This observation suggests that the steel box used in the experiment had negligible sound transmission, indicating its suitability for the experiment. This result is validated by the numerical analysis of the steel box transmission.

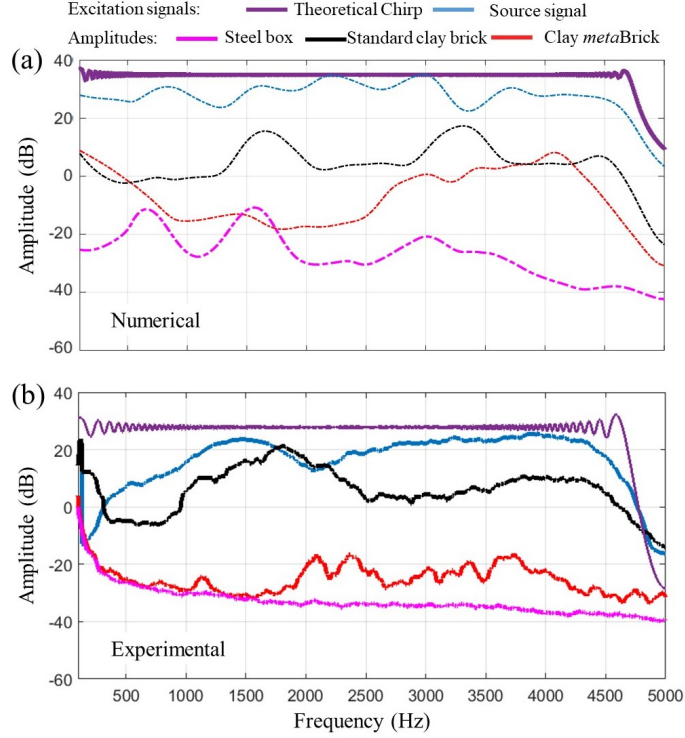


Fig. 8. Acoustic responses: the measured excitation signal is represented by the blue curve, the theoretical excitation chirp signal is represented by the violet curve, the steel box sound transmission is represented by the pink curve, the standard brick sound transmission is represented by the black curve, and the *meta*Brick signal transmission is represented by the red curve. (a) Calculated acoustic responses. (b) Experimental acoustic responses.

The standard brick transmission signal, which showed a high transmission curve compared to the steel box, indicated that the sound transmission through the standard brick was high, with the curve closely following the measured excitation signal. It is clear that the amplitude transmission of the standard brick shows a peak in the vicinity of the frequency of 1500 Hz, which is produced by the reflections inside the steel box. However, the transmission amplitude of the standard brick shows a transmission loss of 20 dB in the band studied in comparison to the measured excitation signal. This finding indicates that the standard brick was not an effective insulator of sound.

In contrast, the *meta*Brick transmission signal showed a very weak transmission curve in contrast to the measured excitation signal and the transmission of the standard brick. The amelioration is based on the presence of the slits in the *meta*Brick, which had excellent performance in the attenuation of the sound at low frequencies. The transmission loss for the wall built on the *meta*Brick up to 40 dB compared to the measured excitation signal and 20 dB compared to the transmission loss generated by the standard brick.

To elaborate further, the thermal study involved measuring the temperature variation inside and outside the iron box over a period of 600 minutes while exposed to a temperature of 90 °C. Inner and outer temperature evolution is measured for both numerical and experimental studies. The results of this study are presented in Fig. 9. It is clearly seen that the numerical and the

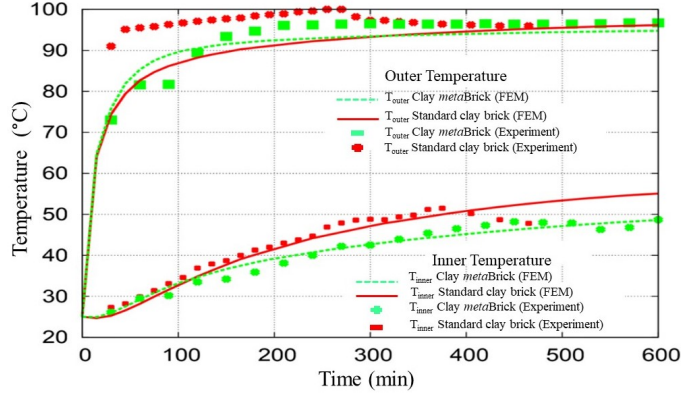


Fig. 9. Numerical and experimental inner and outer temperatures change as a function of exposure time.

experimental results are in good agreement.

The inner temperature variation showed that the *metaBrick* wall was highly effective in thermal insulation, as evidenced by the lower variation of the inner temperature compared to the standard brick. After 600 min of exposure to the outer temperature, as one can see, the standard brick wall exhibited a temperature variation of up to 55 °C (38% of reduction), while the *metaBrick* wall exhibited an inner temperature of up to 48.5 °C (46% of reduction). Thus, make a difference of 6.5 °C, which is equivalent to 8% as a rate of thermal reduction. Furthermore, the outer temperature variation was also significantly lower than that of the standard brick, indicating its effectiveness in thermal insulation.

4. Discussion

To compare the acoustic and thermal properties of the *metaBrick* with a standard brick, we used finite element simulations and experimental measurements. We found that the presence of the slits in the *metaBrick* design created a barrier, which effectively reduced the sound transmission and heat diffusion. The presence of the Helmholtz resonators in the *metaBrick* design allowed for the dissipation of sound and heat energy, reducing the amplitude of the transmitted waves. This is in contrast to a standard brick, which does not have the ability to attenuate sound or heat in this way. The acoustic insulation becomes higher with a sound transmission of up to 20 dB in the frequency range of 200 Hz to 3.5 kHz. The same occurs for the thermal insulation, which became more efficient with a rate of 8% compared with the standard brick. Moreover, bricks are usually subjected to compression loads. As a result, understanding the compressive strength of bricks is of the utmost significance for establishing their suitability for construction.

We conducted both numerical and experimental compression tests on the *metaBrick* and standard clay brick. Fig. 10 shows the numerical compression stress-strain curve and the mechanical resistance of bricks during compression, which is measured using a compression testing machine. Besides, experimentally we examined four samples of each type of brick and determined their compressive strength in MPa. The results of the study are summarized in Table 2.

The standard brick has an average compressive strength of around 19 MPa, whereas the *metaBrick* has an average compressive strength of about 12 MPa. Although *metaBrick* has lost strength, it

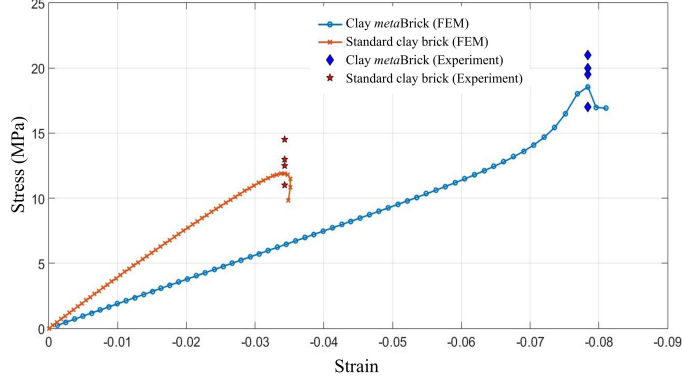


Fig. 10. The numerical compression stress-strain curve is in line, and the experimental compressive strength is in dashed points for both standard brick and *metabrick*.

still possesses a relatively high compressive strength that is more than enough for the building sector (7.5 MPa) [40]. The reason for the strength loss is due to the existence of slits in *metaBrick*, which causes the compressive strength to decrease by approximately 7 MPa, which is equivalent to 33% when compared with standard brick.

Table 2: Compressive strength of bricks.

Type of brick	Sample	Compressive strength (MPa)	Average compressive strength
Standard clay brick	1	19.5	19.37
	2	17	
	3	21	
	4	20	
Clay <i>metabrick</i>	1	11	12.75
	2	14.5	
	3	12.5	
	4	13	

This *metaBrick* results in more comfortable and environmentally friendly buildings, reducing energy consumption and noise transmission in the construction industry, and is easy to manufacture by just adding some steel beams to the existing molds in the industries. The presence of the Helmholtz resonators in the *metaBrick* design allows for a significant reduction in sound transmission and thermal conductivity, making it a promising candidate for use in building materials applications. These findings can be useful for researchers, designers, and engineers who seek to develop more sustainable and environmentally friendly building materials that offer better acoustic and thermal insulation properties.

The concept of metamaterials is a relatively new path in material design, and our study shows that it has immense potential for revolutionizing the construction industry. The use of metamaterials can pave the way for the development of more sustainable and energy-efficient building materials, leading to a reduction in energy consumption and a more comfortable building environment. Our study’s findings have significant practical implications and can contribute to the development of

innovative solutions for the construction sector.

5. Conclusions

In conclusion, the present study has investigated the acoustic and thermal behaviors of a novel metamaterial design named *metaBrick*. Numerical simulations and experimental measurements have demonstrated that the presence of slits in alveoli in the *metaBrick* structure creates Helmholtz resonators, which can effectively attenuate both sound and heat. The findings of this study indicate that *metaBrick* has a strong potential for improving insulation performance in building materials with a compressive strength that is high enough for the construction sector. The results also indicate that further research is warranted to explore the use of metamaterials in multi-functional applications to enhance building performance and energy efficiency. Overall, this study has demonstrated the importance of developing new and innovative building materials to meet the increasing demand for sustainable and energy-efficient buildings. Metamaterials, such as the *metaBrick* design, have shown potential for making significant contributions to this effort.

Acknowledgements

We would like to thank the Moroccan Ministry of Higher Education, Scientific Research and Innovation and the OCP Foundation who funded this work through the APRD research program.

References

- [1] M. M. Al-Humaiqani, S. G. Al-Ghamdi, The built environment resilience qualities to climate change impact: Concepts, frameworks, and directions for future research, *Sustainable Cities and Society* (2022) 103797 [doi:10.1016/j.scs.2022.103797](https://doi.org/10.1016/j.scs.2022.103797).
- [2] J. Wang, B. Du, Y. Huang, Experimental study on airborne sound insulation performance of lightweight double leaf panels, *Applied Acoustics* 197 (2022) 108907. [doi:10.1016/j.apacoust.2022.108907](https://doi.org/10.1016/j.apacoust.2022.108907).
- [3] F. Anjum, M. Y. Naz, A. Ghaffar, K. Kamran, S. Shukrullah, S. Ullah, Sustainable insulating porous building materials for energy-saving perspective: Stones to environmentally friendly bricks, *Construction and Building Materials* 318 (2022) 125930. [doi:10.1016/j.conbuildmat.2021.125930](https://doi.org/10.1016/j.conbuildmat.2021.125930).
- [4] Y. Gao, X. Meng, A comprehensive review of integrating phase change materials in building bricks: Methods, performance and applications, *Journal of Energy Storage* 62 (2023) 106913. [doi:10.1016/j.est.2023.106913](https://doi.org/10.1016/j.est.2023.106913).
- [5] M. Sutcu, J. J. del Coz Díaz, F. P. Á. Rabanal, O. Gencel, S. Akkurt, Thermal performance optimization of hollow clay bricks made up of paper waste, *Energy and Buildings* 75 (2014) 96–108. [doi:10.1016/j.enbuild.2014.02.006](https://doi.org/10.1016/j.enbuild.2014.02.006).
- [6] M. Fringuellino, R. Smith, Sound transmission through hollow brick walls, *Building acoustics* 6 (3) (1999) 211–224. [doi:10.1260/1351010991501419](https://doi.org/10.1260/1351010991501419).

- [7] D. Vijayan, A. Mohan, J. Revathy, D. Parthiban, R. Varatharajan, Evaluation of the impact of thermal performance on various building bricks and blocks: A review, *Environmental Technology & Innovation* 23 (2021) 101577. doi:10.1016/j.eti.2021.101577.
- [8] P. Principi, R. Fioretti, Thermal analysis of the application of pcm and low emissivity coating in hollow bricks, *Energy and Buildings* 51 (2012) 131–142. doi:10.1016/j.enbuild.2012.04.022.
- [9] M. Mahdaoui, S. Hamdaoui, A. A. Msaad, T. Kousksou, T. El Rhafiki, A. Jamil, M. Ahachad, Building bricks with phase change material (pcm): Thermal performances, *Construction and Building Materials* 269 (2021) 121315. doi:10.1016/j.conbuildmat.2020.121315.
- [10] Z. Aketouane, M. Malha, D. Bruneau, A. Bah, B. Michel, M. Asbik, O. Ansari, Energy savings potential by integrating phase change material into hollow bricks: The case of moroccan buildings, in: *Building Simulation*, Vol. 11, Springer, 2018, pp. 1109–1122. doi:10.1007/s12273-018-0457-5.
- [11] Y. Chihab, R. Bouferra, M. Garoum, M. Essaleh, N. Laaroussi, Thermal inertia and energy efficiency enhancements of hollow clay bricks integrated with phase change materials, *Journal of Building Engineering* 53 (2022) 104569. doi:10.1016/j.jobe.2022.104569.
- [12] A. Bachir, N. Taieb, Numerical analysis for energy performance optimization of hollow bricks for roofing. case study: Hot climate of algeria, *Construction and Building Materials* 367 (2023) 130336. doi:10.1016/j.conbuildmat.2023.130336.
- [13] N. Hichem, S. Noureddine, S. Nadia, D. Djamila, Experimental and numerical study of a usual brick filled with pcm to improve the thermal inertia of buildings, *Energy Procedia* 36 (2013) 766–775. doi:10.1016/j.egypro.2013.07.089.
- [14] Z. Luo, X. Liu, Q. Yang, Z. Qu, H. Xu, D. Xu, Numerical study on performance of porous brick roof using phase change material with night ventilation, *Energy and Buildings* 286 (2023) 112972. doi:10.1016/j.enbuild.2023.112972.
- [15] P. Santos, C. Martins, E. Julio, Enhancement of the thermal performance of perforated clay brick walls through the addition of industrial nano-crystalline aluminium sludge, *Construction and Building Materials* 101 (2015) 227–238. doi:10.1016/j.conbuildmat.2015.10.058.
- [16] G. Jacques, S. Berger, V. Gibiat, P. Jean, M. Villot, S. Ciukaj, A homogenised vibratory model for predicting the acoustic properties of hollow brick walls, *Journal of Sound and Vibration* 330 (14) (2011) 3400–3409. doi:10.1016/j.jsv.2011.02.015.
- [17] C. F. N. Souza, F. Pacheco, M. F. Oliveira, R. F. Heissler, B. F. Tutikian, Impact sound insulation of floor systems with hollow brick slabs, *Case Studies in Construction Materials* 13 (2020) e00387. doi:10.1016/j.cscm.2020.e00387.
- [18] A. S. Al-Tamimi, M. A. Al-Osta, O. S. B. Al-Amoudi, R. Ben-Mansour, Effect of geometry of holes on heat transfer of concrete masonry bricks using numerical analysis, *Arabian Journal for Science and Engineering* 42 (2017) 3733–3749. doi:10.1007/s13369-017-2482-6.
- [19] M. Kadic, G. W. Milton, M. van Hecke, M. Wegener, 3D metamaterials, *Nature Reviews Physics* 2019 1:3 1 (3) (2019) 198–210. doi:10.1038/s42254-018-0018-y.

- [20] N. Gao, Z. Zhang, J. Deng, X. Guo, B. Cheng, H. Hou, Acoustic metamaterials for noise reduction: a review, *Advanced Materials Technologies* 7 (6) (2022) 2100698. doi:[10.1002/admt.202100698](https://doi.org/10.1002/admt.202100698).
- [21] S. A. Cummer, J. Christensen, A. Alù, Controlling sound with acoustic metamaterials, *Nature Reviews Materials* 1 (3) (2016) 1–13. doi:[10.1038/natrevmats.2016.1](https://doi.org/10.1038/natrevmats.2016.1).
- [22] Z. Liu, X. Zhang, Y. Mao, Y. Zhu, Z. Yang, C. T. Chan, P. Sheng, Locally resonant sonic materials, *science* 289 (5485) (2000) 1734–1736. doi:[10.1126/science.289.5485.1734](https://doi.org/10.1126/science.289.5485.1734).
- [23] H. Al Ba’ba’a, M. Nouh, T. Singh, Formation of local resonance band gaps in finite acoustic metamaterials: A closed-form transfer function model, *Journal of Sound and Vibration* 410 (2017) 429–446. doi:[10.1016/j.jsv.2017.08.009](https://doi.org/10.1016/j.jsv.2017.08.009).
- [24] J. Mei, G. Ma, M. Yang, Z. Yang, W. Wen, P. Sheng, Dark acoustic metamaterials as super absorbers for low-frequency sound, *Nature communications* 3 (1) (2012) 1–7. doi:[10.1038/ncomms1758](https://doi.org/10.1038/ncomms1758).
- [25] M. Yang, C. Meng, C. Fu, Y. Li, Z. Yang, P. Sheng, Subwavelength total acoustic absorption with degenerate resonators, *Applied Physics Letters* 107 (10) (2015) 104104. doi:[10.1063/1.4930944](https://doi.org/10.1063/1.4930944).
- [26] H. Zhang, S. Chen, Z. Liu, Y. Song, Y. Xiao, Light-weight large-scale tunable metamaterial panel for low-frequency sound insulation, *Applied Physics Express* 13 (6) (2020) 067003. doi:[10.35848/1882-0786/ab916b](https://doi.org/10.35848/1882-0786/ab916b).
- [27] J.-Y. Jang, C.-S. Park, K. Song, Lightweight soundproofing membrane acoustic metamaterial for broadband sound insulation, *Mechanical Systems and Signal Processing* 178 (2022) 109270. doi:[10.1016/j.ymssp.2022.109270](https://doi.org/10.1016/j.ymssp.2022.109270).
- [28] J. Gu, Y. Tang, X. Wang, Z. Huang, Laminated plate-type acoustic metamaterials with willis coupling effects for broadband low-frequency sound insulation, *Composite Structures* 292 (2022) 115689. doi:[10.1016/j.compstruct.2022.115689](https://doi.org/10.1016/j.compstruct.2022.115689).
- [29] Y. Li, B. M. Assouar, Acoustic metasurface-based perfect absorber with deep subwavelength thickness, *Applied Physics Letters* 108 (6) (2016) 063502. doi:[10.1063/1.4941338](https://doi.org/10.1063/1.4941338).
- [30] X. Cai, Q. Guo, G. Hu, J. Yang, Ultrathin low-frequency sound absorbing panels based on coplanar spiral tubes or coplanar helmholtz resonators, *Applied Physics Letters* 105 (12) (2014) 121901. doi:[10.1063/1.4895617](https://doi.org/10.1063/1.4895617).
- [31] T. Wu, T. Cox, Y. Lam, From a profiled diffuser to an optimized absorber, *The Journal of the Acoustical Society of America* 108 (2) (2000) 643–650. doi:[10.1121/1.429596](https://doi.org/10.1121/1.429596).
- [32] C. Shen, Y. Liu, L. Huang, On acoustic absorption mechanisms of multiple coupled quarter-wavelength resonators: Mutual impedance effects, *Journal of Sound and Vibration* 508 (2021) 116202. doi:[10.1016/j.jsv.2021.116202](https://doi.org/10.1016/j.jsv.2021.116202).
- [33] J. Li, W. Wang, Y. Xie, B.-I. Popa, S. A. Cummer, A sound absorbing metasurface with coupled resonators, *Applied Physics Letters* 109 (9) (2016) 091908. doi:[10.1063/1.4961671](https://doi.org/10.1063/1.4961671).

- [34] N. Jiménez, W. Huang, V. Romero-García, V. Pagneux, J.-P. Groby, Ultra-thin metamaterial for perfect and quasi-omnidirectional sound absorption, *Applied Physics Letters* 109 (12) (2016) 121902. doi:[10.1063/1.4962328](https://doi.org/10.1063/1.4962328).
- [35] N. Jiménez, V. Romero-García, V. Pagneux, J.-P. Groby, Rainbow-trapping absorbers: Broad-band, perfect and asymmetric sound absorption by subwavelength panels for transmission problems, *Scientific reports* 7 (1) (2017) 13595. doi:[10.1038/s41598-017-13706-4](https://doi.org/10.1038/s41598-017-13706-4).
- [36] T. Han, X. Bai, J. T. Thong, B. Li, C.-W. Qiu, Full control and manipulation of heat signatures: cloaking, camouflage and thermal metamaterials, *Advanced Materials* 26 (11) (2014) 1731–1734. doi:[10.1002/adma.201304448](https://doi.org/10.1002/adma.201304448).
- [37] Y. Li, W. Li, T. Han, X. Zheng, J. Li, B. Li, S. Fan, C.-W. Qiu, Transforming heat transfer with thermal metamaterials and devices, *Nature Reviews Materials* 6 (6) (2021) 488–507. doi:[10.1038/s41578-021-00283-2](https://doi.org/10.1038/s41578-021-00283-2).
- [38] Z. Zhang, L. Xu, T. Qu, M. Lei, Z.-K. Lin, X. Ouyang, J.-H. Jiang, J. Huang, Diffusion metamaterials, *Nature Reviews Physics* (2023) 1–18doi:[10.1038/s42254-023-00565-4](https://doi.org/10.1038/s42254-023-00565-4).
- [39] H. Hoppen, F. Langfeldt, W. Gleine, O. von Estorff, Helmholtz resonator with two resonance frequencies by coupling with a mechanical resonator, *Journal of Sound and Vibration* (2023) 117747doi:[10.1016/j.jsv.2023.117747](https://doi.org/10.1016/j.jsv.2023.117747).
- [40] O. Gencel, Characteristics of fired clay bricks with pumice additive, *Energy and Buildings* 102 (2015) 217–224. doi:[10.1016/j.enbuild.2015.05.031](https://doi.org/10.1016/j.enbuild.2015.05.031).